Applied and Environmental Microbiology, Oct. 2010, p. 6455–6462 Vol. 76, No. 19
0099-2240/10/$12.00 doi:10.1128/AEM.00975-10

Boosting Autofermentation Rates and Product Yields with Sodium Stress Cycling: Application to Production of Renewable Fuels by Cyanobacteria▽†

Damian Carrieri,[1]‡ Dariya Momot,[1] Ian A. Brasg,[1] Gennady Ananyev,[1]# Oliver Lenz,[1,2] Donald A. Bryant,[3] and G. Charles Dismukes[1]*

Department of Chemistry and Princeton Environmental Institute, Princeton University, Princeton, New Jersey 08544[1]; Institute of Biology, Humboldt University, Berlin, Germany[2]; and Department of Biochemistry and Molecular Biology, The Pennsylvania State University, University Park, Pennsylvania 16802[3]

Received 21 April 2010/Accepted 28 July 2010

Sodium concentration cycling was examined as a new strategy for redistributing carbon storage products and increasing autofermentative product yields following photosynthetic carbon fixation in the cyanobacterium *Arthrospira* (*Spirulina*) *maxima*. The salt-tolerant hypercarbonate strain CS-328 was grown in a medium containing 0.24 to 1.24 M sodium, resulting in increased biosynthesis of soluble carbohydrates to up to 50% of the dry weight at 1.24 M sodium. Hypoionic stress during dark anaerobic metabolism (autofermentation) was induced by resuspending filaments in low-sodium (bi)carbonate buffer (0.21 M), which resulted in accelerated autofermentation rates. For cells grown in 1.24 M NaCl, the fermentative yields of acetate, ethanol, and formate increase substantially to 1.56, 0.75, and 1.54 mmol/(g [dry weight] of cells · day), respectively (36-, 121-, and 6-fold increases in rates relative to cells grown in 0.24 M NaCl). Catabolism of endogenous carbohydrate increased by approximately 2-fold upon hypoionic stress. For cultures grown at all salt concentrations, hydrogen was produced, but its yield did not correlate with increased catabolism of soluble carbohydrates. Instead, ethanol excretion becomes a preferred route for fermentative NADH reoxidation, together with intracellular accumulation of reduced products of acetyl coenzyme A (acetyl-CoA) formation when cells are hypoionically stressed. In the absence of hypoionic stress, hydrogen production is a major beneficial pathway for NAD^+ regeneration without wasting carbon intermediates such as ethanol derived from acetyl-CoA. This switch presumably improves the overall cellular economy by retaining carbon within the cell until aerobic conditions return and the acetyl unit can be used for biosynthesis or oxidized via respiration for a much greater energy return.

Growth of aquatic microbial oxygenic phototrophs (AMOPs) such as cyanobacteria, algae, and diatoms as renewable feedstocks for energy production has been proposed as an advantageous alternative to growing land-based crops for biofuels (9, 11, 14). These organisms can be grown efficiently on water, sunlight, carbon dioxide, and minimal nutrients on nonarable land or at coastal marine sites. They produce easily digested biopolymers that can be more readily converted to fuels than recalcitrant cellulosic feedstocks. Nevertheless, efficient strategies for converting accumulated biomass from AMOPs into useful fuels are still needed.

One strategy for converting cyanobacterial biomass to liquid and gaseous fuels is to allow these cells to rely on their own fermentative pathways—a process termed "autofermentation." With autofermentation, cells anaerobically catabolize their internally stored carbohydrate molecules (glycogen and soluble sugars), producing CO_2, reductants, and energy as ion gradients and phosphorylation to regenerate ATP. The reducing equivalents in the form of NAD(P)H may be reused by the cell or excreted from the cell as reduced carbon products, typically organic acids and alcohols. The identities of these products are determined by the physiological conditions and by which fermentative enzymes are active. The genomes of cyanobacteria differ in terms of which genes of fermentative enzymes are present and functional, leading to a range of possible fermentative product yields and rates. A major limitation to the technological use of autofermentation for fuel production from biomass is the slow time scale of the conversion in relation to the light/dark cycle of growth.

Two fermentation products useful as fuels that are excreted by some cyanobacteria are ethanol and hydrogen. Ethanol production via autofermentation occurs naturally in some cyanobacteria (22). Genetic engineering has been applied successfully to establish autofermentative ethanol production in the cyanobacterium *Synechococcus* sp. PCC 7942, which does not produce detectable amounts of ethanol in the wild type (10). This strain was created by insertion of the genes for pyruvate decarboxylase and alcohol dehyrogenase from *Zymomonas mobilis*. Genetic engineering has also been successfully applied to stimulate fermentative hydrogen production in *Synechococcus* sp. PCC 7002 by increasing the level of the limiting cellular

* Corresponding author. Present address: Waksman Institute and Department of Chemistry and Chemical Biology, Rutgers University, Piscataway, NJ 08854. Phone: (732) 445-6786. Fax: (732) 445-5735. E-mail: dismukes@rci.rutgers.edu.

‡ Present address: Biosciences Center, National Renewable Energy Laboratory, Golden, CO 80401.

Present address: Waksman Institute and Department of Chemistry and Chemical Biology, Rutgers University, Piscataway, NJ 08854.

† Supplemental material for this article may be found at http://aem.asm.org/.

▽ Published ahead of print on 6 August 2010.

reductant NADH via disruption of the lactate dehydrogenase gene (19).

For biotechnological applications, the following two goals have been identified for increasing production of autofermentation products and hydrogen by AMOPs (1): (i) increase photoautotrophic accumulation of stored carbohydrates and (ii) increase the catabolic rate of carbohydrates under dark anaerobic conditions. Here we have continued our work with *Arthrospira* (*Spirulina*) *maxima* with efforts to achieve these two goals.

Different approaches for increasing carbohydrate content for cyanobacteria exist. One is nutrient deprivation. Many cyanobacteria, including *Arthrospira* species, do not have nitrogenase (*nif*) genes and therefore require a nitrogen source (such as nitrate, ammonia, or urea) for protein synthesis. Deprivation of a nitrogen source is a well-documented strategy for increasing the glycogen content (stored as insoluble carbohydrate granules) in many nondiazotrophic cyanobacteria (3, 13, 23, 26). Sulfur deprivation has also been shown to increase the glycogen content in at least two cyanobacteria when incubated in the presence of methane (2). Recently, it was demonstrated that sulfur and nitrogen limitation, rather than complete deprivation, provides optimal autofermentative hydrogen yields in the cyanobacterium *Synechocystis* sp. PCC 6803 (5).

A different approach, which increases soluble sugars in cyanobacteria, involves adaptation of cells to media with high concentrations of sodium salts. Many cyanobacteria accumulate organic molecules such as glucosyl-glycerol and/or trehalose to osmotically balance their cytosols with the extracellular medium (6, 17, 20). In addition to glycogen, these molecules can serve as substrates for fermentation in cyanobacteria (22). Both glucosyl-glycerol and trehalose are present in *Arthrospira platensis* (29) and *A. maxima* CS-328 (8). It was shown that a 4-fold increase in carbohydrate content can be achieved by growing *A. platensis* in media supplemented with additional 1 M NaCl relative to no additional NaCl (28).

Acceleration of carbohydrate autofermentation in cyanobacteria by application of selective physiological stresses has been previously proposed (1). Here we report a new strategy that combines the established method for increasing carbohydrate content in *Arthrospira* by adapting filaments to highly saline growth media (28) with hypoionic stress to accelerate autofermentation. The entire process can be described as "sodium stress cycling," which relies on hyperionic conditions (high salt) during growth to accumulate sugars, followed by hypoionic stress (low salt) to force catabolism during autofermentation. By resuspending filaments grown in media containing excess NaCl into buffer containing only sufficient solute to prevent lysis at the start of autofermentation, we achieve a large increase in total fermentative product yields relative to cells that were not adapted to high salt. However, this strategy did not lead to higher hydrogen yields, demonstrating that other fermentative routes (primarily ethanol production) are used for NADH recycling in *A. maxima* under hypoionic conditions.

MATERIALS AND METHODS

Cell culturing. *Arthrospira* (*Spirulina*) *maxima* (CS-328), henceforth referred to as *A. maxima*, was obtained from the Tasmanian CSIRO Collection of Living Microalgae and was grown at 30°C in batch culture in 2.8-liter Roux flasks containing 1 liter of Zarrouk's medium (ZM). ZM consists of sodium (bi)carbonate buffer (pH 9.8) plus additional macro- and micronutrients necessary for growth and autofermentative hydrogen production. All components of ZM have been previously listed elsewhere (7). The final sodium concentration of ZM was 240 mM. Cultures were illuminated by cool white fluorescent lamps, with a light flux of 40 μE m^{-2} s^{-1} on a 12-h light/12-h dark cycle for 14 days. *A. maxima* filaments were harvested by flotation in a separatory funnel and resuspended in 1 liter of fresh modified Zarrouk's medium. This homogenous suspension containing 0.68 g (dry weight) of cells (liter culture)$^{-1}$ was divided into five 200-ml aliquots and set in 1-liter flasks under illumination and temperature conditions as described above. Each flask was subsequently supplemented with 0 to 1.00 M additional sodium chloride added every 2 to 3 days in 0.25 M increments (final growth medium denoted ZM, ZM + 0.25 M NaCl, etc.) and was kept under the same illumination and temperature conditions for a total of 2 additional weeks of growth (e.g., all cultures were grown for exactly 14 additional days after the initial division of the 1-liter culture, including the 2- to 3-day increments during salt additions). Dry weights before and after salt addition were determined by pipetting 20 ml of cells onto preweighed porous filter discs (5 μm pore size; Pall Life Sciences, Ann Arbor, MI), with growth medium removed by suction filtration; the filter discs were then dried at 70°C until constant mass (~2 days) and reweighed. Error in these measurements was estimated at $\pm$0.2 mg per sample.

Polarographic measurements. Following growth of *A. maxima* filaments in ZM + 0 to 1.00 M NaCl, 1-ml aliquots of cultures were taken for polarographic oxygen measurements. Oxygen concentrations were measured from continuously stirred culture aliquots with a Clark-type oxygen electrode (Hansatech Instruments, Norfolk, England), with respect to time in total darkness and in saturating (>1,000 μE m^{-2} s^{-1}) white light. The initial rate of oxygen uptake (taken over 1 min) from culture aliquots in total darkness was inferred to be the respiration rate after correction for baseline drift, which was minimal. The initial rate of increasing oxygen concentration (taken over 2 min) for the same aliquot of culture placed in saturating white light was then determined. The oxygen evolution rate was calculated by subtracting the dark respiration rate from the rate of appearance of oxygen in saturating light. Dark respiration and light-saturated O_2 evolution rates were normalized to the chlorophyll contents of the culture aliquots. Chlorophyll content was determined by extraction in *N*,*N*-dimethylformamide and absorbance at 652 nm with a spectrophotometer, as described previously (4, 7).

Variable fluorescence measurements. Dark- and light-adapted variable fluorescence of filaments was determined from 3-ml aliquots of cultures grown in ZM + 0 to 1.00 M NaCl with a FL-3000 kinetic fluorometer (Photon System Instruments, Czech Republic). For dark-adapted measurements, culture aliquots were placed in total darkness for at least 2 min. The minimum dark-adapted fluorescence (F_0) was then determined by dim probe pulses (9 μs long, 1 s apart). Subsequently, a saturating flash (900 ms) was supplied, and the maximum fluorescence (F_m) of the filaments was measured using a probe pulse of 30 μs after the saturating flash (to avoid interference with the saturating flash). The same sample was then placed under moderate red-orange light (~50 μE m^{-2} s^{-1}) for 5 min, and analogous F_0 and F_m measurements were taken (denoted F_0' and F_m', respectively) in the presence of this light. Dark-adapted variable fluorescence is thus measured $F_v/F_m = (F_m - F_0)/F_m$, and light-adapted variable fluorescence is thus measured $F_v'/F_m' = (F_m' - F_0')/F_m'$.

Carbohydrate determination. The total carbohydrate fractions were determined from filament suspensions in growth media based on an adapted anthrone method that was developed for whole-cell suspensions of yeast (25) and has been applied to studies of *Arthrospira* whole filaments by others (24). Cell suspensions (100 μl) were added to 900 μl anthrone reagent solution (consisting of 0.2 g anthrone per 100 ml of 71% sulfuric acid in water) and heated at 100°C for 10 min. The resulting solution was measured in a spectrophotometer. The absorbance at 620 nm was compared against a calibration curve prepared with glucose standards ranging from 10 to 50 μg glucose per 100 μl solution. In one experiment, the anthrone method was used to determine the carbohydrate content in cells before and after autofermentation, and the difference was inferred to be the total carbohydrate catabolized. Total "glucose equivalents" consumed were determined by measuring the carbohydrate content before and after fermentation by this method.

Insoluble glycogen was determined in parallel samples of cell suspensions with a method similar to that reported by Ernst et al. (12). Cell suspensions (100 μl) were added to 200 μl of 48% KOH and incubated at 100°C for 1 h. Subsequently, 600 μl of cold (0°C) absolute ethanol was added, and this suspension was centrifuged at 13,000 $\times$ *g*. The supernatant was discarded, and the pellet was washed twice with cold ethanol. Water (100 μl) and 900 μl anthrone reagent solution were added to the pellet. This solution was heated for 10 min at 100°C and measured with a spectrophotometer as described above. A calibration curve

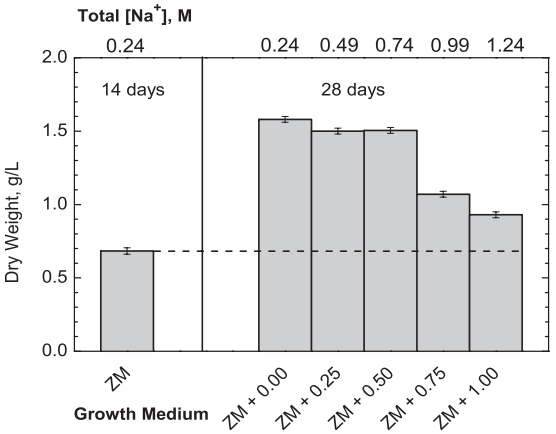

FIG. 1. Accumulated biomass of *A. maxima* filaments after light-limited growth in variable concentrations of sodium chloride, added to ZM (total sodium content, 0.24 M). *A. maxima* was initially grown to a cell density of 0.7 g (dry weight) of cells (liter culture)$^{-1}$ for 14 days. Subsequently, filaments were resuspended at this concentration in fresh Zarrouk's medium supplemented with 0 to 1.00 M additional sodium chloride, added every 2 to 3 days in 0.25 M increments, and the dry weights of cultures were measured 2 weeks after initial division of the 1-liter cultures. Light intensity equaled 40 μE m^{-2} s^{-1}, with 12 h light/12 h dark. Data were obtained from single dry weight measurements, with propagated estimated errors.

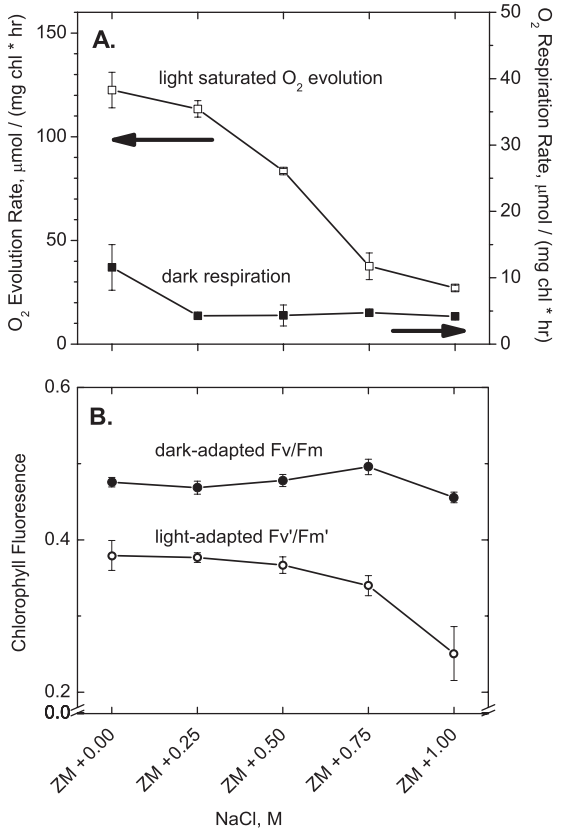

FIG. 2. Effect of salt stress on light-saturated oxygen evolution, dark respiration, and variable fluorescence of *A. maxima* filaments. (A) The disappearance of soluble oxygen from suspensions of *A. maxima* filaments was measured in total darkness to determine the respiration rates. The appearance of oxygen in light-saturating conditions (>1,000 μE m^{-2} s^{-1} white light) minus the magnitude of the dark consumption rate (respiration) determined the light-saturated O_2 evolution rates. Note the different *y*-axis scales. chl, chlorophyll. (B) Suspensions of *A. maxima* filaments were adapted in darkness for at least 2 min before determining the average dark-adapted variable fluorescence (F_v/F_m). Light-adapted variable fluorescence (F_v'/F_m') was determined after 5 min of exposure to moderate light (~50 μE m^{-2} s^{-1} red-orange light). Note the offset *y* axis. Data display the means ± 1 standard deviation from three measurements.

prepared with bovine glycogen (Sigma) had the same slope as one prepared with glucose (not shown), and calibration curves prepared with trehalose and sucrose had slopes that were double of that of the calibration curve prepared glucose on a molar basis (not shown).

Cell autofermentation. *A. maxima* filaments were harvested from ZM + 0 to 1.00 M NaCl by suction filtration onto porous filter discs (5 μm pore size; Pall Life Sciences, Ann Arbor, MI) and resuspended in sodium (bi)carbonate buffer (BC) consisting of 7.0 g (66 mM) Na_2CO_3 and 6.5 g (77.4 mM) $NaHCO_3$ per liter, with a final Na^+ concentration of 210 mM at pH 9.8. BC is the same buffer as that used in ZM but lacks macro- and micronutrient additions (which includes an additional 30 mM $NaNO_3$). In one experiment, BC was supplemented with 0.5 M NaCl (denoted BC + 0.5 M NaCl), resulting in a final Na^+ concentration of 0.71 M. Cells were suspended in BC at cell densities equivalent to those used after growth (0.75 to 1.5 g liter^{-1}). Aliquots (3 ml) of these suspensions were pipetted into small glass vials (10 ml, total volume). Vials were subsequently sealed with Teflon-coated rubber septa and covered with aluminum foil for darkness, and the headspace in each vial was purged with argon gas to induce micro-oxic conditions. Dissolved oxygen in the cell suspension was consumed by respiration, yielding full anaerobiosis, as confirmed by oximetry using a Clark electrode on replicate samples (data not shown). Vials were incubated at 30°C under these dark anaerobic conditions for up to 2 days.

Fermentation product measurements. Hydrogen in the headspace above the cultures was monitored by withdrawing 200-μl headspace samples with a gastight syringe (Hamilton) and injecting them in a calibrated gas chromatograph (Gow-Mac) equipped with a 13× molecular sieve column and argon carrier gas.

Following hydrogen measurements, vials were opened, and *A. maxima* cell suspensions were immediately passed through prewashed 0.2-μm syringe filters (Whatman, Florham Park, NJ). The resulting cell-free solutions were collected in Eppendorf tubes. A total of 540 μl of the solution was pipetted into Pyrex nuclear magnetic resonance (NMR) tubes (New Era Enterprises, Inc., Vineland, NJ), to which 60 μl of D_2O containing 30 μg/ml TSP [3-(trimethylsilyl)propionic-2,2,3,3-D_4 acid sodium salt] (Sigma-Aldrich) was added, and tubes were mixed by inversion and vortexing. Water-soluble end products were then measured by ^1H nuclear magnetic resonance spectroscopy as described elsewhere (8). We should note that our method assumes that the major fractions of organic acids and alcohols are not retained intracellularly during fermentation. In other cyanobacteria, there is reasonable carbon balance between catabolized sugars (glycogen) and excreted product measurements (22, 27).

RESULTS

Aerobic photoautotrophic growth of filaments in increasing salt concentrations led to decreased photosynthetic biomass yields. Figure 1 shows the initial cell densities of cultures before and after addition of 0 to 1.00 M NaCl plus 2 weeks of growth. While cells grown in Zarrouk's medium (ZM) plus 0 to 0.50 M NaCl had similar final cell densities, the addition of 0.75 and 1.00 M NaCl clearly decreased the final yield. This decrease in biomass yield may reflect either reduced photosynthetic capacity or elevated respiration rate, or both. The difference between the sum of the light-saturated photosynthetic and respiratory electron transport rates and the dark respiration rate, as measured by the light-saturated oxygen evolution rate (Fig. 2A), decreases significantly for cells grown in ZM + 0.25 M NaCl and higher. The lack of quantitative correlation between light-limited biomass yield (at 40 μE m^{-2} s^{-1}) and the initial light-saturated O_2 evolution rate (>1,000 μE m^{-2} s^{-1})

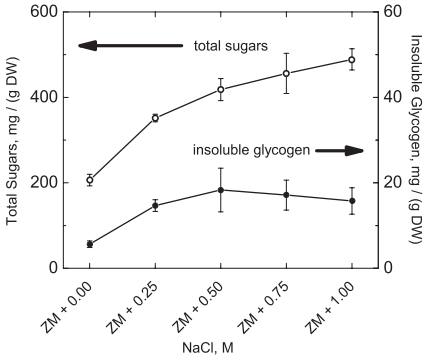

FIG. 3. Total sugar and insoluble glycogen contents of *A. maxima* filaments adapted to variable concentrations of sodium chloride. The total sugar content increased from ~200 to ~500 mg/g (dry weight) of cells (~20% to ~50% of dry weight content) when incubated in Zarrouk's medium with an additional 0 to 1 M NaCl. Insoluble glycogen was a very small component of total sugars (<0.2% dry weight), indicating that salt stress induced an increase primarily in the cellular content of soluble sugars. Note the different *y*-axis scales. Data display the means ± 1 standard deviation from three measurements. DW, dry weight.

likely reflects the different kinetic limitations imposed under these distinct light regimes. Thus, while salt-induced retardation in photosynthetic electron transport from water to CO_2 occurs at saturating light intensities, it does not impose a kinetic block on biomass yield at the lower light intensity. The chlorophyll fluorescence emission yield reflects the quantum efficiency of photosystem II (PSII) charge separation (16). When measured using cells adapted to continuous light, similar to growth conditions (50 $\mu E\ m^{-2}\ s^{-1}$), it was found to decrease with increasing salt concentration (Fig. 2B) in parallel with the biomass yield (Fig. 1). This appears to arise from the same kinetic block that limits light-driven O_2 evolution. In contrast, salt addition does not appreciably affect the variable fluorescence yield of filaments that are dark adapted (Fig. 2A), indicating a fully functional PSII that is not affected. We conclude that electron or proton transport rates downstream of PSII impose a kinetic block as the salt concentrations in the growth medium increase, and this effect can be revealed at saturating light intensities.

Total sugars normalized to the dry weights of filaments increased significantly upon supplementation with sodium chloride. In all cases, less than 5% of total sugars were in the form of insoluble sugars that precipitated in 67% cold ethanol (Fig. 3). Total sugars increased from about 20% of the filaments' dry weight when grown in ZM with no additional NaCl to almost 50% of the dry weight when grown in ZM + 1.00 M NaCl.

Cells that had been grown in higher NaCl concentrations showed no significant increase in autofermentative hydrogen production (normalized to the dry weight), as shown in Fig. 4A. However, other fermentative products, including ethanol,

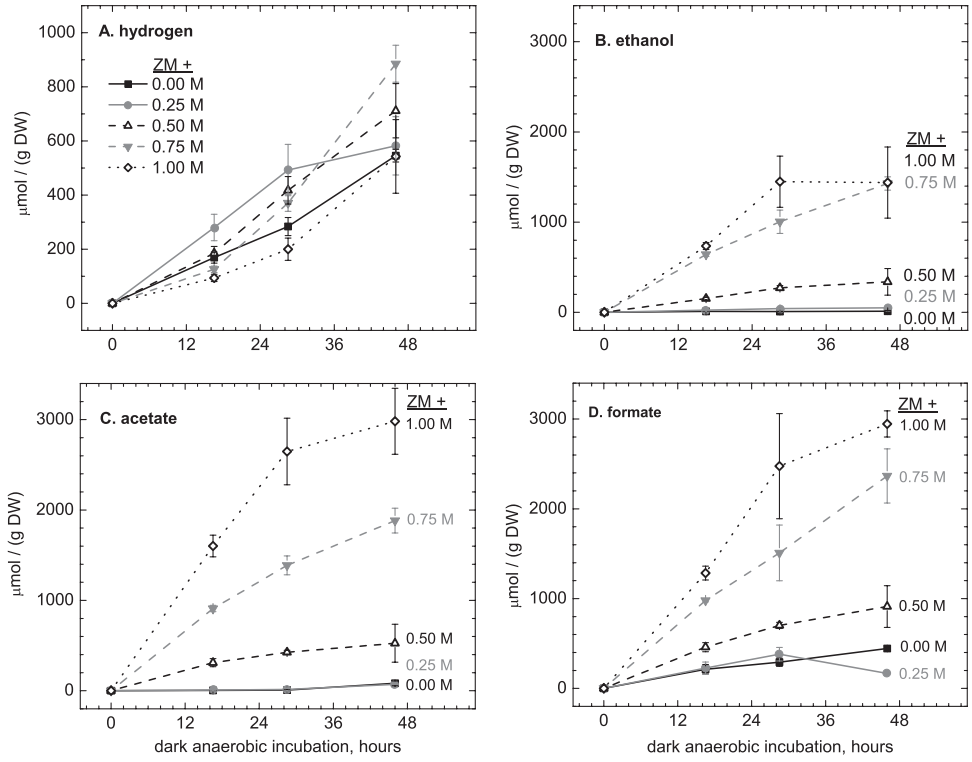

FIG. 4. (A to D) Effect of sodium cycling on major fermentation product yields from *A. maxima* filaments under autofermentative conditions for 0 to 2 days. Filaments were grown in Zarrouk's medium with an additional 0.00, 0.25, 0.50, 0.75, or 1.00 M NaCl; subsequently, filaments were resuspended in 210 mM sodium (bi)carbonate buffer, pH 9.8, and incubated under dark anaerobic conditions to induce osmotic stress (see Materials and Methods). The cells underwent autofermentation to produce hydrogen (A), ethanol (B), acetate (C), and formate (D). Lactate was only a minor fermentative product and was never detected in amounts higher than 150 µmol (g [dry weight] of cells)$^{-1}$. Data display the means ± 1 standard deviation from three measurements.

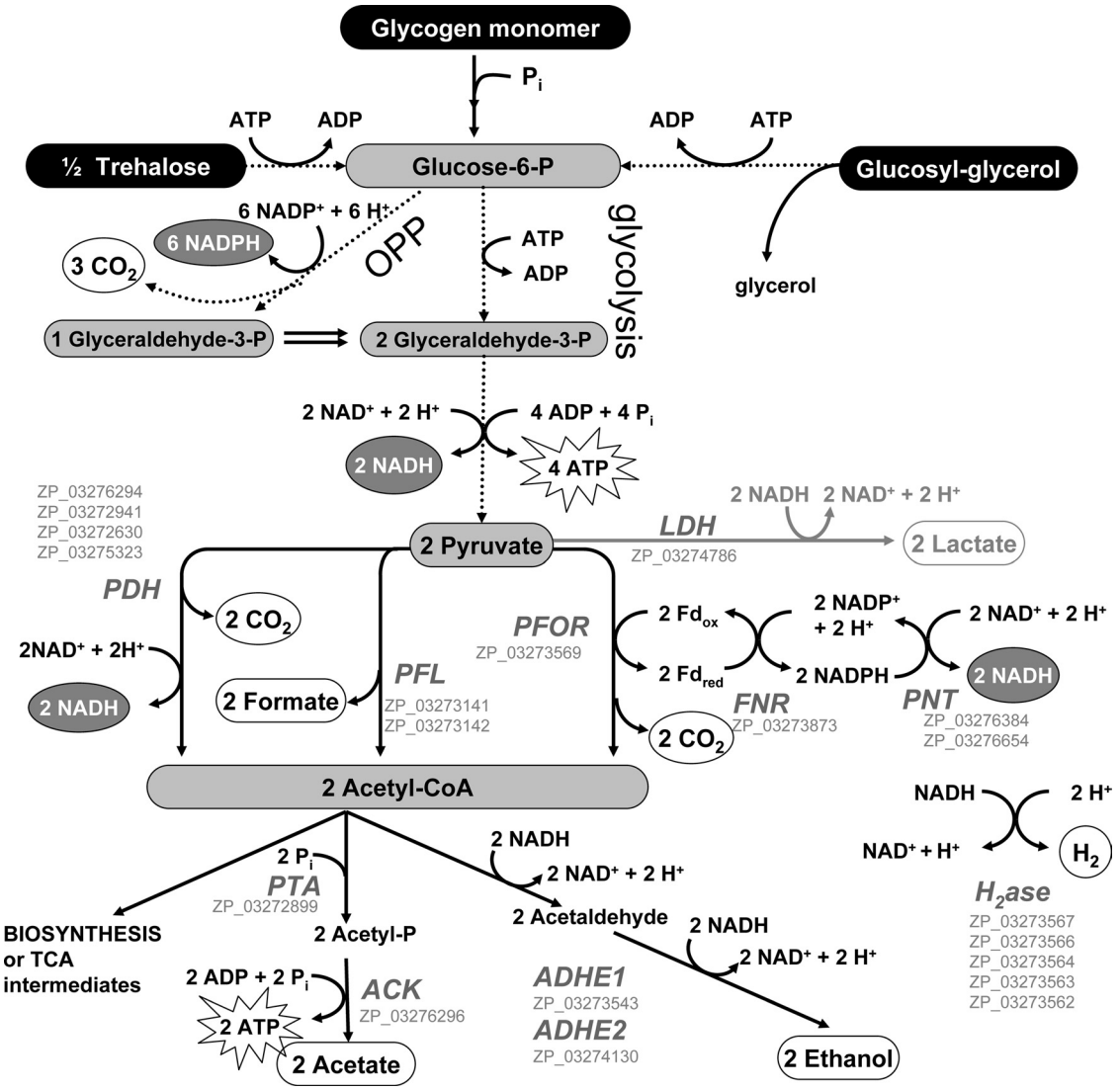

FIG. 5. Proposed autofermentative scheme for *A. maxima* based on observed excreted products (white circles), previously observed substrates (black circles) (8), and identified enzymes present in the *A. maxima* genome (GenBank accession numbers [gray letters]). Pathways with multiple steps (glycolysis and oxidative pentose phosphate [OPP] pathways) are given as dotted lines. Lactate production is provided in gray because it was a minor end product for all experiments in this study. Enzyme abbreviations: LDH, lactate dehydrogenase; PDH, pyruvate dehydrogenase; PFL, pyruvate formate lyase; PFOR, pyruvate ferredoxin oxidoreductase; FNR, ferredoxin NADP reductase; PNT, pyridine NADH transhydrogenase; PTA, phosphotransacetylase; ACK, acetate kinase; ADHE, bifunctional aldehyde alcohol dehydrogenase; H_2ase, hydrogenase. The enzymes required for the glycolysis and OPP pathways and the biosynthetic/degradation pathways for trehalose and glucosyl-glycerol were identified in the *A. maxima* genome (see the supplemental material for annotation of the glucosyl-glycerol, trehalose, and glycogen pathways).

acetate, and formate, increased significantly (Fig. 4B to D). The initial rates of excretion of these products were also higher, as seen by increased initial slopes of the time course experiment data (Fig. 4B to D). Lactate was sometimes observed in trace amounts but did not exceed 150 μmol (g [dry weight] cells)$^{-1}$ in any sample. Otherwise, no other excreted fermentative products were observed in cell-free media by proton NMR in any autofermentation experiment presented in this report (detection limit < 50 μM). Hydrogen yield was not limited by the headspace partial pressure, as dissolved hydrogen rates were also measured on an electrode that continuously consumes dissolved hydrogen (1), and yielded similar hydrogen rates regardless of hypoionic stress (see Fig. S1 in the supplemental material).

In Fig. 5, we present a diagram of the carbohydrate metabolic pathways deduced from the measured end products and the enzymes deduced from the draft genome of *A. maxima*. The observed large increase in total fermentative product yields with increasing hypoionic stress requires that there was an increase in total carbohydrate catabolism with increasing hypoionic stress. Assuming that 1 glucose-6-phosphate is converted through the Embden-Meyerhof pathway to 2 equivalents of pyruvate, followed by complete excretion of pyruvate-derived products acetate, lactate, and ethanol, one

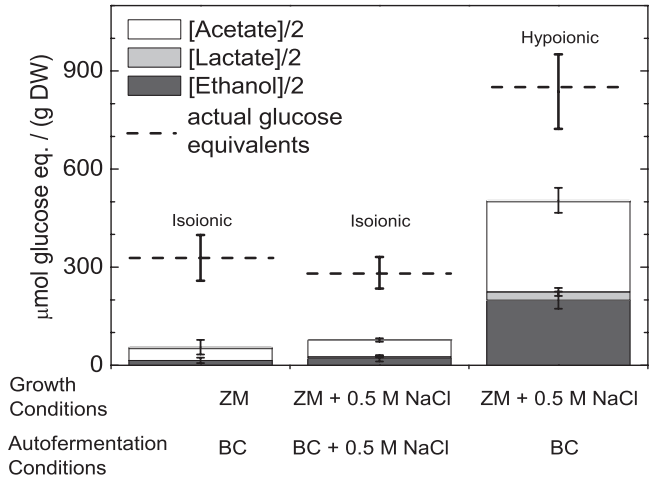

FIG. 6. Effect of hypoionic conditions on carbohydrate catabolism of *A. maxima* filaments under autofermentative conditions for 1 day. Cells were grown in Zarrouk's medium (ZM) either with or without additional 0.5 M NaCl. Subsequently, cells were harvested and suspended in bicarbonate buffer (BC) with or without 0.5 M NaCl. Stacked columns show the amounts of excreted products after 1 day of autofermentation divided by 2 to represent how many glucose equivalents (eq.) were catabolized to produce these products via glycolysis. Each column represents the minimal amount of glucose equivalents that must have fermented to yield such values. The actual total carbohydrate content consumed (based on the measured carbohydrate content of filaments before and after 1 day of autofermentation) is displayed as a dashed line. Assuming solely a glycolysis model, if every mole of glucose consumed led to an excreted product, the sum of the stacked values and dashed line value would be equal. Assuming solely an oxidative pentose phosphate (OPP) model, if every mole of glucose consumed led to an excreted product, the sum of the stacked values would equal exactly half of the value of the dashed line. Data display the means ± 1 standard deviation from three measurements.

can calculate the amount of glucose equivalents catabolized in the cell by dividing the sum of the fermentative products by two. Note that this assumes no involvement of the oxidative pentose phosphate pathway, which is discussed later. This calculated value can be compared to the actual amount of measured glucose equivalents in the cell before and after fermentation (an experimental measurement of carbohydrate consumed by the cell).

Figure 6 displays these data for three cases, as follows: (i) cells grown in ZM and autofermented for 1 day in BC (isoionic); (ii) cells grown in ZM + 0.5 M NaCl and autofermented for 1 day in BC + 0.5 M NaCl (isoionic); and (iii) cells grown ZM + 0.5 M NaCl and autofermented for 1 day in BC (hypoionic). Concentrations of excreted acetate, lactate, and ethanol, divided by two, are shown as a stacked bar graph in units of "glucose equivalents," representing the amount of carbohydrate that must have been consumed to produce the observed excreted products. The actual amount of carbohydrate consumed, determined from the difference of measured carbohydrate content before and after autofermentation, is shown as a dashed line.

For cells autofermented in buffers isoionic with those of their growth media (cases i and ii described above) a small percentage (<30%) of actual glucose equivalents consumed can be accounted for by the excreted products acetate, lactate, and ethanol. No significant difference in total excreted products or actual consumed glucose equivalents is observed between cases i and ii. However, case iii (hypoionic) lead to an ~5-fold increase in total excreted products and an ~2-fold increase in actual carbohydrates consumed. In the latter case, approximately 50% of consumed carbohydrate was converted into excreted products by fermentation. Thus, hypoionic stress not only results in an increase of fermentative products formation but also accelerates sugar catabolism.

We now note that Fig. 5 also accounts for possible involvement of the oxidative pentose phosphate (OPP) pathway. Some cyanobacteria have been concluded to follow a mixture of both glycolysis and oxidative pentose phosphate (OPP), followed by fermentation (22, 27). A modified stoichiometry can be calculated, assuming 100% of consumed carbohydrate is catabolized via the OPP pathway. Assuming that 1 glucose-6-phosphate is converted through the OPP pathway to 1 pyruvate (plus 3 CO_2), followed by complete excretion of the pyruvate-derived products acetate, lactate, and ethanol, the calculated amount of glucose equivalents catabolized in the cell would be the sum of these fermentative products. Because we were unable to measure CO_2 in these experiments, we cannot easily differentiate between these two pathways and therefore give only limits of stoichiometries of 100% OPP or 100% glycolysis, with the reality likely being somewhere in between.

Thus, in Fig. 6, the stacked values multiplied by two would give the theoretical amount of glucose equivalents catabolized if the OPP pathway was utilized entirely. Note that even in this case, the amount of excreted fermentative products for cells without hypoionic stress (cases i and ii) cannot account entirely for the measured amount of glucose equivalents catabolized.

DISCUSSION

Salt stress has a pronounced effect on photosynthetic efficiency. The final biomass yields from cells grown in ZM + 0.75 M NaCl and ZM + 1.00 M NaCl were clearly lower relative to cultures grown in ZM + 0 to 0.50 M NaCl (Fig. 1). Vonshak et al. reported a nearly linear decrease in growth rates with respect to added NaCl (also from 0 to 1.00 M) when growing a similar salt-tolerant strain, *Arthrospira platensis*, at a light intensity double of that used under our growth conditions (80 versus 40 $\mu E\ m^{-2}\ s^{-1}$) (28). They reported that this effect was correlated with a decrease in light-dependent oxygen evolution when assaying photosynthesis under high light (700 $\mu E\ m^{-2}\ s^{-1}$). We also saw a decrease in light-dependent oxygen evolution under light-saturating conditions (>1,000 $\mu E\ m^{-2}\ s^{-1}$), as illustrated in Fig. 2A, but saw no correlation between salt stress and dark-adapted variable fluorescence (Fig. 2B, black solid circles). Variable fluorescence (F_v/F_m) measures the efficiency of photosystem II (PSII) charge separation under single-turnover conditions isolated from that of other downstream electron transport reactions that may influence the PSII turnover rate. Because added salt does not affect F_v/F_m in dark-adapted cells, it is concluded that salt stress does not specifically inhibit PSII charge separation. Instead, the photosynthetic electron transport chain must be inhibited downstream of PSII, thereby lowering the PSII turnover rate. This is confirmed by measuring F_v/F_m in light-adapted cells (termed (F_v'/F_m') (Fig. 2B, open circles) under light intensity similar to

that used under growth conditions (~50 μE m^{-2} s^{-1}). In these measurements, the yield of charge separation of PSII is expected to decrease, owing to the accumulation of reduced electron transport carriers downstream of PSII (6). The observed decrease in F_v'/F_m' follows the same trend as that of the decrease in growth shown in Fig. 1. Under low-light-intensity growth conditions, we observed significant inhibition of photosynthesis only with 0.75 or 1.00 M additional NaCl, with little effect on photosynthetic efficiency for cultures supplemented with 0.50 M NaCl or less. However, given the measurements of light-saturated oxygen evolution and the results of Vonshak et al., we would expect to see inhibited growth of cultures supplemented with even less NaCl if grown under higher ambient light. This is significant because ambient sunlight can reach very high photon fluxes (1,500 μE m^{-2} s^{-1}).

A key advantage of growing cells in higher salt is demonstrated by the 2.5-fold increase in soluble sugar content (percent dry weight), as illustrated in Fig. 3. Filaments grown in ZM with no additional NaCl contained 20% (200 mg [g {dry weight} of cells]$^{-1}$) sugars by dry weight, while cells grown in ZM + 1.00 M NaCl yielded nearly 50% sugar by dry weight. In all cases, over 95% of these sugars are classified "soluble," as they did not precipitate upon addition of cold ethanol, which occurs for glycogen (12). High-salt conditions during photoautotrophic growth of algae and cyanobacteria are known to induce the accumulation of osmolytes, which protect cells from dehydration (15, 17). Both glucosyl-glycerol and trehalose are known to be salt induced in *Arthrospira platensis* (29), and we have confirmed the presence of these "osmoprotectants" in aqueous cell lysate fractions of *A. maxima* by ^{13}C NMR (8) and confirmed the presence of the genes for their synthesis in the genome (see the supplemental material). We believe that these sugars are the dominant components of the "soluble" sugar fraction that we measured using the anthrone assay.

Biofuel research has developed technologies emphasizing the conversion of carbohydrates or lipids to useable fuels. Most cyanobacteria do not make significant levels of neutral lipids (14), and consequently, methods for increasing sugar content and improving the conversion of biomass to ethanol or hydrogen are of keen interest. Here, we demonstrate that increasing the carbohydrate pool size by inducing the synthesis of soluble sugars rather than polymeric glycogen produces a precursor that can more efficiently be converted by autofermentation into products including ethanol. Some strains of cyanobacteria, such as *Oscillatoria* and *Microcoleus*, have been shown to accumulate osmoprotectants that can serve as fermentative substrates (22).

We anticipated that hypoionic stress of hypersaline-grown filaments during autofermentation would increase the rates of carbohydrate catabolism, possibly due to changes in osmotic pressure or the Na^+ ion potential across cell membranes. Cells grown in high salt (ZM + 1.00 M NaCl) experienced a significant (>1 M) change in ionic strength between growth and autofermentative conditions. This indeed causes significant increases in excreted ethanol, acetate, and formate (Fig. 4B to D). However, hydrogen production is relatively unchanged (Fig. 4A). We infer that hydrogen production is unaffected because none of the additional NADH that must be produced by the greatly increased rate of carbon metabolism (Fig. 6) is available to or utilized by the bidirectional hydrogenase enzyme. Rather, the excess reductant capacity is partially excreted as soluble fermentation products, particularly as formate but also as ethanol (Fig. 4). The major fraction of the reductant capacity from catabolized carbohydrate is not excreted as organic acids or alcohol but is retained in the cell in a new (polymeric?) form that is not soluble and not detected by the anthrone assay (Fig. 6). A possible candidate fitting this description could be polyhydroxybutyrate (PHB), although we did not attempt to measure cell extracts for this compound in this work.

We note also that significant formate and hydrogen production occurred even for cultures that were grown at lower salt (ZM + 0 to 0.25 M NaCl), whereas very little acetate or ethanol was observed for cells under these conditions (Fig. 4). Thus, at lower salt concentrations, the bulk of the reductant flux that is excreted appears as formate, thus requiring the production of an equivalent flux of acetyl coenzyme A (acetyl-CoA) and its utilization in nonmonitored pathways (biosynthesis and tricarboxylic acid [TCA]). This conclusion is also supported by the observation that more glucose equivalents are catabolized during autofermentation than can be accounted for by the excreted products of cells autofermented in isotonic buffer (Fig. 6).

Figure 5 represents a working model for metabolic pathways for glycolysis, oxidative pentose phosphate, and pyruvate fermentation predicted from the draft genome of *A. maxima* (http://genome.ornl.gov/microbial/amax/) and corroborated by the present and previous data from NMR-detected metabolites (8). The genome draft has at least 99% sequence coverage of the completed genome and is thus useful for assembling this model.

The quantitative accounting of catabolized carbohydrates when applied to the pathways shown in Fig. 5 documents an important rerouting of carbon that has not been proposed in other cyanobacterial fermentation pathways, to our knowledge (22). Namely, acetyl-CoA generated from pyruvate is converted to excreted products such as ethanol or acetate (as is also observed in other cyanobacteria) but a significant amount is retained in the cell, perhaps in the form of acetyl-CoA itself or more likely in the forms of downstream intermediates in the TCA cycle or biosynthetic products. Accumulation of acetyl-CoA produces equivalent increases in either NADH or reduced ferredoxin (Fd) via the pyruvate dehydrogenase (PDH) and pyruvate ferredoxin oxidoreductase (PFOR) pathways, respectively, and thus could be expected to activate pathways for reductive assimilation of carbon or elimination of H_2 (hydrogenase mediated) to maintain redox balance. As noted, H_2 is not affected in *A. maxima*. In contrast, the significant increase in excreted formate via the pyruvate formate lyase (PFL) enzyme in *A. maxima* enables accumulation of acetyl-CoA without the build-up of NADH, reduced Fd, or the products which they produce. The PFL pathway is not widespread in cyanobacteria and algae (see Table S1 in the supplemental material). We found 5 out of 28 cyanobacterial genomes in the CyanoBase database and 5 out of 190 algal genomes in the NCBI database which contain both *pflA* (structural gene) and *pflB* (activating cofactor). The structural genes for the bidirectional [NiFe]-hydrogenase are found in all five of these cyanobacteria.

This retention of C_2 carbon (acetyl) coupled to the excretion

of reduced C_1 carbon (formate) via the PFL pathway is more economical on a carbon basis than excretion of acetate and ethanol via conventional fermentation and could potentially be beneficial to the cells. Cells that can store acetyl units would be better equipped for ATP production and/or biosynthesis upon the return of aerobic conditions (which would be brought about by light in oxygenic phototrophs or upon mixing in air). For cells that are under hypoionic stress during anaerobiosis, a larger fraction of acetyl-CoA should be converted to excreted fermentation products as a means to reduce the osmotic potential, since the forced catabolism of one osmotically active sugar molecule would produce two osmotically active pyruvate molecules. Thus, the observed preferential increase in the fractions of excreted acetate, lactate, and ethanol over formate (Fig. 6) under higher hypotonic stress may be a mechanism to lower the osmotic potential while regenerating the NAD^+ required to maintain glycolytic ATP production.

This "osmotic hypothesis" might offer further insight into why some cyanobacteria produce hydrogen as a product but not under hypoionic stress. Hydrogen production offers a mechanism for cyanobacteria, such as *Arthrospira*, to regenerate NAD^+ from glycolysis-derived NADH without loss of valuable carbon units (acetyl-CoA equivalents). In contrast, in the case when cells are hypotonically stressed (a widely encountered environmental condition for hypersaline AMOPs) and more acetyl-CoA equivalents are being produced, ethanol excretion allows for regeneration of NAD^+ from NADH while also lowering the intracellular osmotic potential, thus leading to observed increases in ethanol production rather than hydrogen production. Measurements of intracellular metabolite pools after induction of dark anaerobisis by liquid chromatography coupled to mass spectrometry might further support the "osmotic hypothesis."

This study has addressed the effects of sodium stress cycling but not necessarily those of osmotic stress caused by other osmolytes. For example, in *Synechocystis* sp. PCC 6803, it was shown that the response to solutes used to induce hypertonic (hyperosmotic) stress differs depending on the identity of the solute used (18). Although the same systems are involved in transduction of salt signals and hyperosmotic signals, expression of individual genes is regulated to different extents when using sodium chloride versus sorbitol in this organism (21). It would be interesting to compare the effects of sodium stress cycling with the effects of cycling a different solute such as sorbitol on autofermentative yields.

ACKNOWLEDGMENTS

This work was supported by an AFOSR-MURI grant (FA9550-05-1-0365). We acknowledge fellowship support by the NSF REU (to D.M.) and support by the Deutsche Forschungsgemeinschaft through Sfb498 and the Cluster of Excellence "UniCat" (to O.L.).

We thank L. T. Guerra and K. McNeely for providing genomic search results and Amaya Garcia-Costas for culturing *A. maxima* for genomic DNA.

REFERENCES

1. **Ananyev, G., D. Carrieri, and G. C. Dismukes.** 2008. Optimization of metabolic capacity and flux through environmental cues to maximize hydrogen production by the cyanobacterium "*Arthrospira* (*Spirulina*) *maxima*." Appl. Environ. Microbiol. **74:**6102–6113.
2. **Antal, T. K., and P. Lindblad.** 2005. Production of H_2 by sulphur-deprived cells of the unicellular cyanobacteria *Gloeocapsa alpicola* and *Synechocystis* sp. PCC 6803 during dark incubation with methane or at various extracellular pH. J. Appl. Microbiol. **98:**114–120.
3. **Aoyama, K., I. Uemura, J. Miyake, and Y. Asada.** 1997. Fermentative metabolism to produce hydrogen gas and organic compounds in a cyanobacterium, *Spirulina platensis*. J. Ferment. Bioeng. **83:**17–20.
4. **Arnon, D. I.** 1949. Copper enzymes in isolated chloroplasts—polyphenoloxidase in *Beta vulgaris*. Plant Physiol. **24:**1–15.
5. **Burrows, E. H., F. W. R. Chaplen, and R. L. Ely.** 2008. Optimization of media nutrient composition for increased photofermentative hydrogen production by *Synechocystis* sp. PCC 6803. Int. J. Hydrogen Energy **33:**6092–6099.
6. **Campbell, D., V. Hurry, A. K. Clarke, P. Gustafsson, and G. Oquist.** 1998. Chlorophyll fluorescence analysis of cyanobacterial photosynthesis and acclimation. Microbiol. Mol. Biol. Rev. **62:**667–683.
7. **Carrieri, D., G. Ananyev, A. M. Garcia Costas, D. A. Bryant, and G. C. Dismukes.** 2008. Renewable hydrogen production by cyanobacteria: nickel requirements for optimal hydrogenase activity. Int. J. Hydrogen Energy **33:**2014–2022.
8. **Carrieri, D., K. McNelly, A. C. De Roo, N. Bennette, I. Pelczer, and G. C. Dismukes.** 2009. Identification and quantification of water-soluble metabolites by cryoprobe-assisted nuclear magnetic resonance spectroscopy applied to microbial fermentation. Magn. Reson. Chem. **47:**S138–S146.
9. **Chisti, Y.** 2007. Biodiesel from microalgae. Biotechnol. Adv. **25:**294–306.
10. **Deng, M. D., and J. R. Coleman.** 1999. Ethanol synthesis by genetic engineering in cyanobacteria. Appl. Environ. Microbiol. **65:**523–528.
11. **Dismukes, G. C., D. Carrieri, N. Bennette, G. M. Ananyev, and M. C. Posewitz.** 2008. Aquatic phototrophs: efficient alternatives to land-based crops for biofuels. Curr. Opin. Biotechnol. **19:**235–240.
12. **Ernst, A., H. Kirschenlohr, J. Diez, and P. Boger.** 1984. Glycogen content and nitrogenase activity in *Anabaena variabilis*. Arch. Microbiol. **140:**120–125.
13. **Gorl, M., J. Sauer, T. Baier, and K. Forchhammer.** 1998. Nitrogen-starvation-induced chlorosis in *Synechococcus* PCC 7942: adaptation to long-term survival. Microbiology **144**(Pt. 9)**:**2449–2458.
14. **Hu, Q., M. Sommerfeld, E. Jarvis, M. Ghirardi, M. Posewitz, M. Seibert, and A. Darzins.** 2008. Microalgal triacylglycerols as feedstocks for biofuel production: perspectives and advances. Plant J. **54:**621–639.
15. **Kirst, G. O.** 1990. Salinity tolerance of eukaryotic marine algae. Annu. Rev. Plant Physiol. **41:**21–53.
16. **Kolber, Z. S., O. Prasil, and P. G. Falkowski.** 1998. Measurements of variable chlorophyll fluorescence using fast repetition rate techniques: defining methodology and experimental protocols. Biochim. Biophys. Acta **1367:**88–106.
17. **Mackay, M. A., R. S. Norton, and L. J. Borowitzka.** 1984. Organic osmoregulatory solutes in cyanobacteria. J. Gen. Microbiol. **130:**2177–2191.
18. **Marin, K., M. Stirnberg, M. Eisenhut, R. Kramer, and M. Hagemann.** 2006. Osmotic stress in *Synechocystis* sp. PCC 6803: low tolerance towards nonionic osmotic stress results from lacking activation of glucosylglycerol accumulation. Microbiology **152:**2023–2030.
19. **McNeely, K., Y. Xu, N. Bennette, D. A. Bryant, and G. C. Dismukes.** 2010. Redirecting reductant flux into hydrogen production via metabolic engineering of fermentative carbon metabolism in a cyanobacterium. Appl. Environ. Microbiol. **76:**5032–5038.
20. **Reed, R. H., L. J. Borowitzka, M. A. Mackay, J. A. Chudek, R. Foster, S. R. C. Warr, D. J. Moore, and W. D. P. Stewart.** 1986. Organic solute accumulation in osmotically stressed cyanobacteria. FEMS Microbiol. Rev. **39:**51–56.
21. **Shoumskaya, M. A., K. Paithoonrangsarid, Y. Kanesaki, D. A. Los, V. V. Zinchenko, M. Tanticharoen, I. Suzuki, and N. Murata.** 2005. Identical Hik-Rre systems are involved in perception and transduction of salt signals and hyperosmotic signals but regulate the expression of individual genes to different extents in *Synechocystis*. J. Biol. Chem. **280:**21531–21538.
22. **Stal, L. J., and R. Moezelaar.** 1997. Fermentation in cyanobacteria. FEMS Microbiol. Rev. **21:**179–211.
23. **Stevens, S. E., D. L. Balkwill, and D. A. M. Paone.** 1981. The effects of nitrogen limitation on the ultrastructure of the cyanobacterium *Agmenellum quadruplicatum*. Arch. Microbiol. **130:**204–212.
24. **Tadros, M. G., and R. D. MacElroy.** 1988. Characterization of *Spriulina* biomass for *CELSS Diet Potential*. NASA-CR-185329, NASA contractor NCC 2–501. Alabama A&M University, Normal, AL.
25. **Trevelyan, W. E., and J. S. Harrison.** 1952. Studies on yeast metabolism. I. Fractionation and microdetermination of cell carbohydrates. Biochem. J. **50:**298–303.
26. **Troshina, O., L. Serebryakova, M. Sheremetieva, and P. Lindblad.** 2002. Production of H-2 by the unicellular cyanobacterium *Gloeocapsa alpicola* CALU 743 during fermentation. Int. J. Hydrogen Energy **27:**1283–1289.
27. **van der Oost, J., B. A. Bulthuis, S. Feitz, K. Krab, and R. Kraayenhof.** 1989. Fermentation metabolism of the unicellular cyanobacterium *Cyanothece* PCC 7822. Arch. Microbiol. **152:**415–419.
28. **Vonshak, A., R. Guy, and M. Guy.** 1988. The response of the filamentous cyanobacterium *Spirulina platensis* to salt stress. Arch. Microbiol. **150:**417–420.
29. **Warr, S. R. C., R. H. Reed, J. A. Chudek, R. Foster, and W. D. P. Stewart.** 1985. Osmotic adjustment in *Spirulina platensis*. Planta **163:**424–429.